J. Biochem. 2010;147(5):651–659 doi:10.1093/jb/mvp207

JB THE JOURNAL OF BIOCHEMISTRY

Regulation of alternative splicing of the receptor for advanced glycation endproducts (RAGE) through G-rich *cis*-elements and heterogenous nuclear ribonucleoprotein H

Received December 6, 2009; accepted December 13, 2009; published online December 21, 2009

Kazuyo Ohe[1], Takuo Watanabe[1,*], Shin-ichi Harada[2], Seiichi Munesue[1], Yasuhiko Yamamoto[1], Hideto Yonekura[3] and Hiroshi Yamamoto[1]

[1]Department of Biochemistry and Molecular Vascular Biology, Kanazawa University Graduate School of Medical Science, Kanazawa 920-8640, Japan; [2]Center for Biomedical Research and Education, Kanazawa University Graduate School of Medical Science, Kanazawa 920-8640, Japan; and [3]Department of Biochemistry, Kanazawa Medical University School of Medicine, Uchinada 920-0293, Japan

*Takuo Watanabe, Department of Biochemistry and Molecular Vascular Biology, Kanazawa University Graduate School of Medical Science, 13-1 Takara-machi, Kanazawa, 920-8640, Japan. Tel: +81-076-265-2181, Fax: +81-076-234-4217, E-mail: takuo@med.kanazawa-u.ac.jp

Receptor for advanced glycation endproducts (RAGE) is a cell-surface receptor. The binding of ligands to membrane-bound RAGE (mRAGE) evokes cellular responses involved in various pathological processes. Previously, we identified a novel soluble form, endogenous secretory RAGE (esRAGE) generated by alternative 5′ splice site selection in intron 9 that leads to extension of exon 9 (exon 9B). Because esRAGE works as an antagonistic decoy receptor, the elucidation of regulatory mechanism of the alternative splicing is important to understand RAGE-related pathological processes. Here, we identified G-rich *cis*-elements within exon 9B for regulation of the alternative splicing using a RAGE minigene. Mutagenesis of the G-rich *cis*-elements caused a drastic increase in the esRAGE/mRAGE ratio in the minigene-transfected cells and in loss of binding of the RNA motif to heterogenous nuclear ribonucleoprotein (hnRNP) H. On the other hand, the artificial introduction of a G-stretch in exon 9B caused a drastic decrease in the esRAGE/mRAGE ratio accompanied by the binding of hnRNP H to the RNA motif. Thus, the G-stretches within exon 9B regulate RAGE alternative splicing via interaction with hnRNP H. The findings should provide a molecular basis for the development of medicines for RAGE-related disorders that could modulate esRAGE/mRAGE ratio.

Keywords: alternative splicing/endogenous secretory RAGE (esRAGE)/G-stretch/heterogenous nuclear ribonucleoprotein (hnRNP) H/receptor for advanced glycation endproducts (RAGE).

Abbreviations: AGE, advanced glycation endproducts; esRAGE, endogenous secretory RAGE; hnRNP, heterogenous nuclear ribonucleoprotein; mRAGE, membrane-bound RAGE; qRT-PCR, quantitative reverse transcription PCR; RAGE, receptor for AGE; REMSA, RNA electrophoretic mobility shift assay; RIP, RNA immunoprecipitation.

Alternative splicing is one of the mechanisms that eukaryotes have developed to generate a wider diversity of gene products. In humans, as much as 74% of all genes are estimated to employ this particular mechanism (*1*). The functions of protein products and consequent cellular phenotypes can also be regulated by alternative splicing. In some cases, alternative splicing even yields protein variants with reciprocal functions (*2*), such as signal-transducing agonistic membrane receptors versus their antagonistic decoy counterpart. The production of physiologically antagonistic variants by alternative splicing applies to the pre-mRNA of receptor for advanced glycation endproducts (RAGE), which experiences alternative 5′ splice site selection in intron 9 to produce membrane-bound RAGE (mRAGE) or endogenous secretory RAGE (esRAGE) (*3*, *4*). mRAGE is a multi-ligand receptor that has an extracellular region, consisting of a V-type and two C-type immunoglobulin-like domains, a transmembrane region and a short C-terminal intracellular portion (*5*, *6*). The V-domain of RAGE is critical for the binding of various ligands, including advanced glycation endproducts (AGE) (*5*, *6*), S100 (*7*), amyloid β (*8*), Mac-1 (*9*) and high-mobility group box-1 (HMGB1)/amphoterin (*10*, *11*). The intracellular signals evoked by the binding of these ligands have been implicated in diabetic vascular complications (*12*, *13*), proinflammatory reactions (*6*, *9*), neurodegenerative disorders (*8*) and cancer (*11*). Human esRAGE was identified through an analysis of vascular cell-derived polysomal RNA to be a soluble-form splice variant of RAGE (*3*), which is produced by the utilization of an alternative downstream 5′ splice site in intron 9 that leads to the extension of exon 9 and skipping of exon 10. The extended 82-nucleotide sequence of exon 9, which is designated as exon 9B, contains an in-frame stop codon and gives a unique amino-acid sequence to the C-terminus of esRAGE that lacks the transmembrane domain (Fig. 1). esRAGE is considered to act as a modulating factor opposing the mRAGE-associated conditions in various diseases mentioned above. In fact, accumulating evidence indicates that in patients with some diseases, such as atherosclerosis and diabetic retinopathy, plasma esRAGE levels are significantly lower than

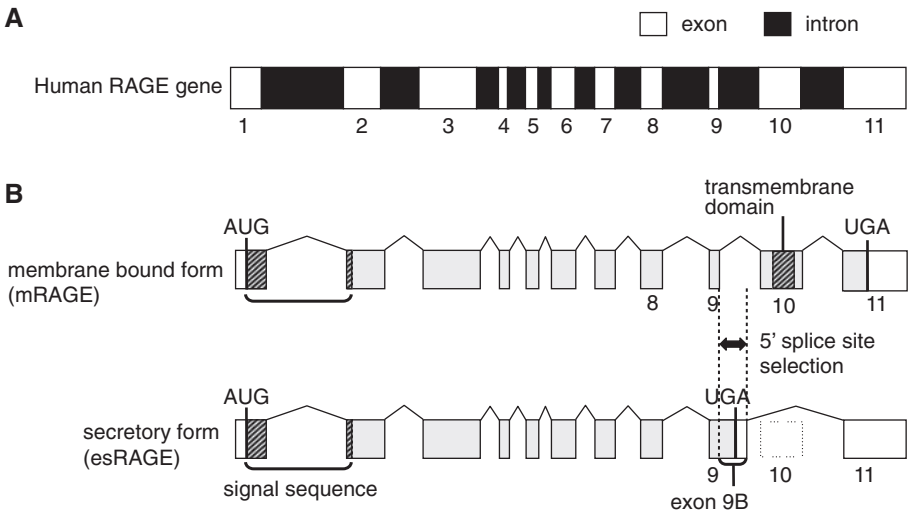

Fig. 1 Schematic representation of the human RAGE gene and its alternative splicing products. (A) Organization of the human RAGE gene (*16*). Open and closed boxes indicate exons and introns, respectively. (B) The membrane-bound form of RAGE (mRAGE) and the secretory form of RAGE (esRAGE). Hatched boxes indicate the signal sequence and transmembrane domain, and shaded boxes indicate the coding regions of the mRNA. These alternatively spliced mRNAs are generated by alternative 5′ splice site selection in intron 9.

those in control groups (*14*, *15*), and supports the view that low levels of circulating esRAGE may cause vulnerability to these diseases. Therefore, elucidation of the regulatory mechanism would provide a molecular basis for the development of drugs that can induce cytoprotective esRAGE but suppress cytotoxic mRAGE. Here, we investigated the molecular mechanisms for regulation of the RAGE alternative splicing by mutagenesis approach using a RAGE minigene.

In the present study, we identified G-rich *cis*-elements within exon 9B, which are essential for the preferential utilization of the upstream mRAGE 5′ splice site. Furthermore, we demonstrated that heterogenous nuclear ribonucleoprotein (hnRNP) H binds to *cis*-elements in a G-stretch-dependent manner. These results suggested that the functions of the *cis*-elements are mediated through interaction with cellular hnRNP H. Taken together, these results suggested that the binding of hnRNP H to G-stretches in exon 9B of RAGE pre-mRNA causes preferential utilization of the upstream mRAGE 5′ splice site in intron 9.

Experimental procedures

Cells

Human microvascular endothelial cells (HMVEC) (KURABO) were maintained in HuMedia-MV2 (KURABO), in accordance with the supplier's instructions, in humidified incubators containing 5% CO_2. The human embryonic kidney cell-derived cell line HEK293T was maintained in Dulbecco's modified Eagle's medium (Nissui) supplemented with 10% foetal bovine serum, penicillin (100 IU/ml) and streptomycin (100 μg/ml).

Antibodies

esRAGE-specific rabbit polyclonal antibody was raised against the unique C-terminal 16-amino-acid peptide (*3*). mRAGE-specific rabbit polyclonal antibody was raised against 17-amino-acid peptide (amino acids 364–380, QRRQRRGEERKAPENQE) that corresponded to the cytoplasmic domain. These antibodies were affinity purified. Anti-GFP rabbit polyclonal antibody from Abcam, anti-hnRNP H rabbit polyclonal antibody from Bethyl Laboratories, anti-hnRNP H goat polyclonal antibody and anti-GAPDH monoclonal antibody from Santa Cruz Biotechnology were purchased.

Construction of RAGE minigene

A RAGE minigene was constructed by insertion of a 3′ part of the human RAGE genomic sequence and a fragment coding for the human RAGE signal sequence into a mammalian expression plasmid pEGFP-N1 (Clontech). PCR amplification of RAGE genomic sequence was accomplished using the cosmid clone KS71 (*16*) as a template, which was kindly provided by Prof. Toshimichi Ikemura (Nagahama Institute of Bio-Science and Technology, Nagahama, Japan). A RAGE genomic sequence from the 3′ part of exon 8 to the 3′ flanking region of exon 11 (nucleotides 8572–9960 of GenBank D28769), including the polyadenylation signal, was amplified and inserted in-frame 3′ to the very end of the EGFP-coding region of pEGFP-N1 using restriction enzymes BsrGI and AflII. For amplification of the fragment coding for the human RAGE signal sequence (nucleotides 1–101 of GenBank AB036432), the full-length RAGE cDNA (*3*) was used as a template and the amplified fragment was inserted into pEGFP-N1 in-frame using restriction enzymes EcoRI and AgeI in the multiple cloning site at 5′ of EGFP-coding region (Fig. 2). Three-nucleotide substitutions were introduced by PCR in accordance with the procedures described previously (*17*). All amplified inserts were sequence-verified. (The primer sequences are listed in Supplementary Table SI).

Transfection

HEK293T cells were transfected with RAGE minigene constructs using FuGENE 6 (Roche). HMVEC were transfected with RAGE minigene constructs using a Microporator MP-100 electroporation device (Digital Bio Technology) following the manufacturer's instructions. Briefly, trypsinized HMVEC cells were washed with PBS, pelleted and resuspended in the Resuspension Solution supplied by the manufacturer. RAGE minigene constructs were added to the cell suspension and mixed well. Then, transient electrical pulses optimized for HMVEC were applied to the cell–DNA mixture in an electrode tip on the device followed by immediate transfer to complete growth medium. Forty-eight hours after transfection, the cells were examined for the production of RAGE splice variants by western blotting or quantitative reverse transcription PCR (qRT–PCR).

Western Blotting

Forty-eight hours after transfection, HMVEC or HEK293T cells were washed with cold PBS, then cells were lysed immediately in SDS-polyacrylamide gel electrophoresis (PAGE) sample buffer [62.5 mM Tris–HCl (pH 6.8), 2% SDS and 10% glycerol]. After

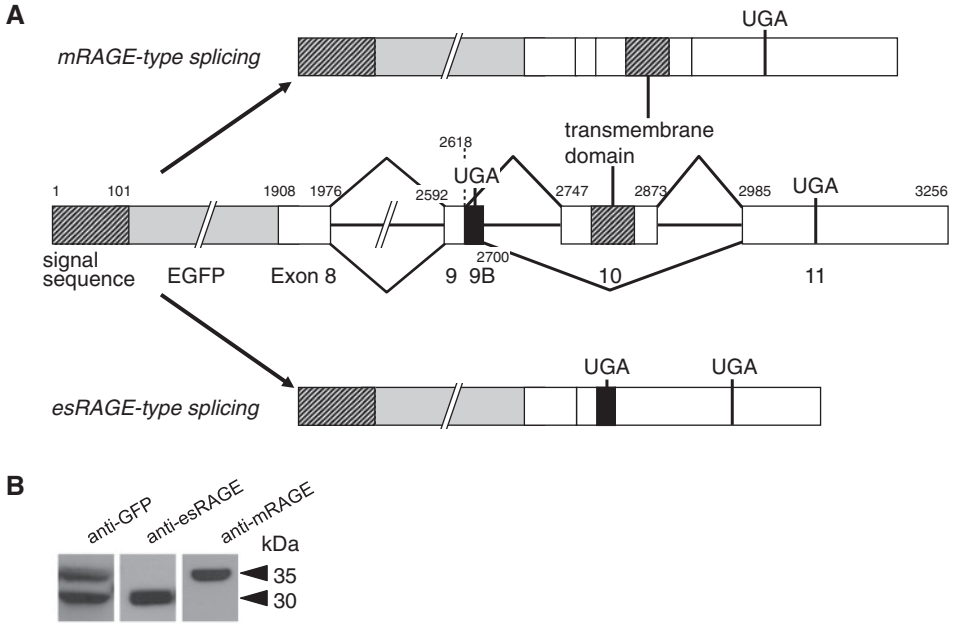

Fig. 2 RAGE minigene construct and its products. (A) Human RAGE minigene construct and the mRAGE- and esRAGE-type products. Middle panel shows a schematic representation of the EGFP-human RAGE fusion minigene. Hatched boxes indicate the signal sequence and transmembrane domain. Shaded boxes indicate the coding sequence for EGFP. Black boxes indicate exon 9B. The first and last nucleotides of RAGE exons are numbered (the nucleotide numbers are based on the genomic sequence starting from the first ATG of exon 1). Top and bottom panels show mRNA products generated by mRAGE-type splicing and esRAGE-type splicing, respectively. (B) Representative western blot of minigene-transfected HEK293T cell lysate. Anti-GFP antibody detected both type products. The anti-esRAGE antibody raised against the unique C-terminal sequence of esRAGE specifically detected the esRAGE-type product. The anti-mRAGE antibody raised against the cytoplasmic domain of mRAGE specifically detected the mRAGE-type product.

determination of protein concentrations using a BCA protein assay kit (Pierce) using BSA as a standard, dithiothreitol and bromophenol blue were added to final concentrations of 100 mM and 0.001% (w/v), respectively. Cell lysates containing 2 μg protein were resolved by SDS-PAGE, and then transferred onto an Immobilon-FL membrane (Millipore). The membrane was treated with primary antibodies and then incubated with 1:3000 diluted horseradish peroxidase-conjugated anti-rabbit IgG (GE Healthcare). The immunoreactive bands were visualized using an ECL detection system (GE Healthcare) and exposure to X-ray film. For quantification of the intensity of immunoreactive bands, 1:10000 diluted infrared fluorescent dye-labelled anti-rabbit and anti-mouse IgG antibody (LI-COR) were used as secondary antibodies and the immunoreactive bands quantified using an Odyssey infrared fluorescence imaging system (LI-COR).

Quantification of RAGE Splice Variants by Multiplex qRT-PCR

Total RNA was isolated from HMVEC using RNeasy Plus Mini Kit (QIAGEN). The sequences of the primers and probes used for the multiplex qRT-PCR assay are listed in Table I. The probes were labelled with different fluorochromes as follows: the mRAGE probe was labelled with FAM and quenched with Black-Hole-Quencher (BHQ) 1; the esRAGE probe was labelled with Quasar 670 and quenched with BHQ2; the GAPDH probe was labelled with CAL Fluor Orange 560 and quenched with BHQ1. All primers and probes were synthesized by Biosearch Technologies.

For qRT-PCR, total RNA were reverse transcribed in 20 μl of reaction mixture using an AffinityScript QPCR cDNA Synthesis Kit (Stratagene Products Division, Agilent Technologies). For cDNA synthesis, random hexamers were used as primers. The multiplex real-time PCR assay was performed to measure both mRAGE and esRAGE in a total reaction mixture (25 μl) containing 2 μl of cDNA mixture, 12.5 μl of 2 × BrilliantII QPCR Master Mix (Stratagene Products Division, Agilent Technologies), primers and probes.

The probes were designed for the variant-specific exons, and primers were designed for the boundary of common and variant-specific exons. Primer and probe concentrations in qRT-PCR were optimized as follows: 100 nM each for forward and reverse primers for mRAGE and for esRAGE, 900 nM each for forward and reverse primers for GAPDH, 100 nM each for probes for mRAGE and for esRAGE and 200 nM for probe for GAPDH. Amplification and real-time fluorescence detection were performed using a model Mx3005P Real Time QPCR system (Stratagene Products Division, Agilent Technologies) and the following protocol: an initial denaturation and polymerase activation step for 10 min at 95°C, followed by 40 cycles of 95°C for 30 s and 60°C for 1 min. Serial dilution of mRAGE and esRAGE plasmid standards was used to construct each standard curve, and the linear range where the standard curve was not affected by the presence of an excessive amount of counterpart plasmid (esRAGE for mRAGE quantification and mRAGE for esRAGE quantification, respectively) was determined. In this way, four orders of magnitude (1×10^2 to 1×10^6 copies) of the linear range in the presence of 1×10^5 copies of counterpart were able to be defined for the quantification of each product. The mRNA expression levels of mRAGE and esRAGE were normalized using GAPDH.

Table I. Primers and probes used for qRT–PCR.

Primer/probe	Sequence
Forward primer for esRAGE	5′-ggccaactgcaggtgag-3′
Reverse primer for esRAGE	5′-ttttctggggccttccattc-3′
Probe for esRAGE	5′-Quasar 670-cttccctgacttta tcaaacccctcacc-BHQ2-3′
Forward primer for mRAGE	5′-caggctctgtgggaggatc-3′
Reverse primer for mRAGE	5′-ggccttcctctcctctcct-3′
Probe for mRAGE	5′-FAM-acagccgccctgctcattgg-BHQ1-3′
Forward primer for GAPDH	5′-gttcgacagtcagccgcat-3′
Reverse primer for GAPDH	5′-aaatccgttgactccgacctt-3′
Probe for GAPDH	5′-CAL Fluor Orange 560 -tttgcgtcgccagccgagc-BHQ1-3′

Table II. Probes used for REMSA.

Probe	Sequence	Nucleotide number
Site 5 wild-type	5′-aagauagcccccaacacaug-3′	(2649–2668)
Site 5 mutant	5′-aagauagcgggcaacacaug-3′	
Site 6-7 wild-type	5′-ugugacuggggggaugguca-3′	(2667–2686)
Site 6 mutant	5′-ugugacucccgggaugguca-3′	
Site 7 mutant	5′-ugugacugggcccaugguca-3′	
Site 8 wild-type	5′-gucaacaagaaaggaauggu-3′	(2683–2702)
Site 8 mutant	5′-gucaacaacuuaggaauggu-3′	

Mutated nucleotides are underlined. The nucleotide numbers are based on the genomic sequence starting from the first ATG of exon 1.

RNA Immunoprecipitation Followed by RNA Electrophoretic Mobility Shift Assay

The sequences of the infrared fluorescent dye-labelled RNA synthetic oligonucleotides used as probes for the REMSA assay are listed in Table II. Nuclear extracts were prepared from HEK293T cells as described previously (*18*). RNA binding reactions were performed in a final volume of 25 µl containing 400 ng of synthetic RNA oligonucleotides labelled by Alexa Fluor 680 at the 5′ end, 50 µg of nuclear extract, 40 units of RNasin Ribonuclease Inhibitor (Promega) and 11.3 µg of tRNAs (Invitrogen) in buffer composed of 10 mM HEPES, 1 mM dithiothreitol, 120 mM KCl, 3 mM $MgCl_2$ and 5% glycerol. The reaction mixtures were incubated at 4°C for 20 min followed by 7 min of UV cross-linking. After UV cross-linking, the hnRNP H-containing complexes were isolated by immunoprecipitation as follows; the reaction mixture was mixed with 75 µl of PBS containing 0.1% Tween 20 (PBS-T) and incubated with 20 µl of Protein G Sepharose 4 Fast Flow (GE Healthcare) precoated with anti-hnRNP H rabbit polyclonal antibody at 4°C for 2–3 h. The pellets were washed with PBS-T three times and the protein–RNA complexes were eluted by boiling the pellet in SDS-PAGE sample buffer. Control immunoprecipitation was carried out using normal rabbit IgG. Samples were separated by a 10% polyacrylamide gel and were transferred onto an Immobilon-FL membrane (Millipore). The membrane was subjected to western blotting using anti-hnRNP H goat polyclonal antibody and fluorescent secondary antibody whose fluorescence could be discriminated from Alexa Fluor 680 used for the RNA probe. The fluorescent bands were visualized using an Odyssey infrared fluorescence imaging system (LI-COR).

Statistical Analysis

One-way analysis of variance (ANOVA) with Scheffé's *post-hoc* test was used for multiple comparisons.

RESULTS

The RAGE Minigene Replicates RAGE Alternative Splicing

To investigate regulatory elements in the alternative splicing of human RAGE transcripts, we constructed a minigene that contains the RAGE gene segment from the 3′ part of exon 8 to the 3′ flanking region of exon 11 and the EGFP gene, so that they would yield EGFP–RAGE fusion proteins (Fig. 2A). The minigene was transfected into HEK293T cells, and expression levels of mRAGE-type and esRAGE-type splicing products were analysed by western blotting using anti-GFP antibody, mRAGE-specific antibody and esRAGE-specific antibody. As shown in Fig. 2B, both mRAGE- and esRAGE-type splicing products were detected in the minigene-transfected HEK293T cells. Direct fusion of EGFP domain to exon 9 of human RAGE gene resulted in aberrant splicing, and mutagenesis at 3′ splice signal elements in intron 8, such as branch point consensus motif and polypyrimidine tract, resulted in skip of exon 9 (data not shown). These results indicated the necessity of intron 8 for replication of the alternative splicing.

G-Stretches in Exon 9B Function as Cis-Elements for Preferential Utilization of the Upstream mRAGE 5′ Splice Site

We introduced a series of 3-nucleotide substitutions to sites 4–8, purine-rich and pyrimidine-rich sequences in exon 9B of the RAGE minigene construct (Fig. 3A). Using this method, the sequences were mutated without affecting the short distance between the two alternative 5′ splice sites in intron 9, thus minimizing the effects of the distance. The five sites were selected so as not to overlap with the minimal binding site of U1 snRNP (−6 to +10 relative to the splice junction) (*19*, *20*).

Four out of the five mutations in exon 9B had profound impacts on the regulation of RAGE splicing in HEK293T cells (Fig. 3B and C). Mutations replacing G-triplets with C-triplets (mut4, mut6 and mut7) significantly increased the %esRAGE (percentage of esRAGE-type product in the sum of esRAGE-type and mRAGE-type products); 83.1% for mut4, 99.8% for mut6 and 97.8% for mut7, while the value for the wild-type sequence was 70.2%. Especially in the case of mut6, the mRAGE-type product was barely detected. On the other hand, replacement of a C-triplet in the middle of a 5-nucleotide C-stretch by a G-triplet (mut5) caused a drastic decrease in %esRAGE to 9.3%. The effect of mutation of a purine tract GAA to a pyrimidine tract CTT (mut8) was marginal (66.4%).

G-Stretches in Exon 9B Function in HMVEC in the Same Manner as in HEK293T Cells

Next, we investigated whether or not the function of the *cis*-elements were dependent on cell type by introducing the same set of exon 9B-mutated minigenes into primary endothelial cells, HMVEC, because the AGE–RAGE axis in the vascular endothelial cell is considered to be a very important factor in the progression of diabetic angiopathy. To achieve high transfer efficiency in the primary cultured cells, we relied on an MP-100 electroporation device. After optimization of the conditions using pEGFP-N1, EGFP expression in 70% or more of HMVEC was observed (data not shown).

The quantification of the splice variants by western blotting using an anti-GFP antibody showed the %esRAGE (63.0%) of wild-type minigene-transfected cells, which was similar to that of HEK293T (70.2%), and similar effects of each mutation on %esRAGE as in the case of HEK293T cells were observed (Fig. 4A and B). Results of direct fluorescence imaging of the minigene-derived products in cells were consistent with the predominant production of mRAGE-type product from the mut5 minigene and the predominant production of esRAGE-type product from the mut6 minigene (Supplementary Fig. S1).

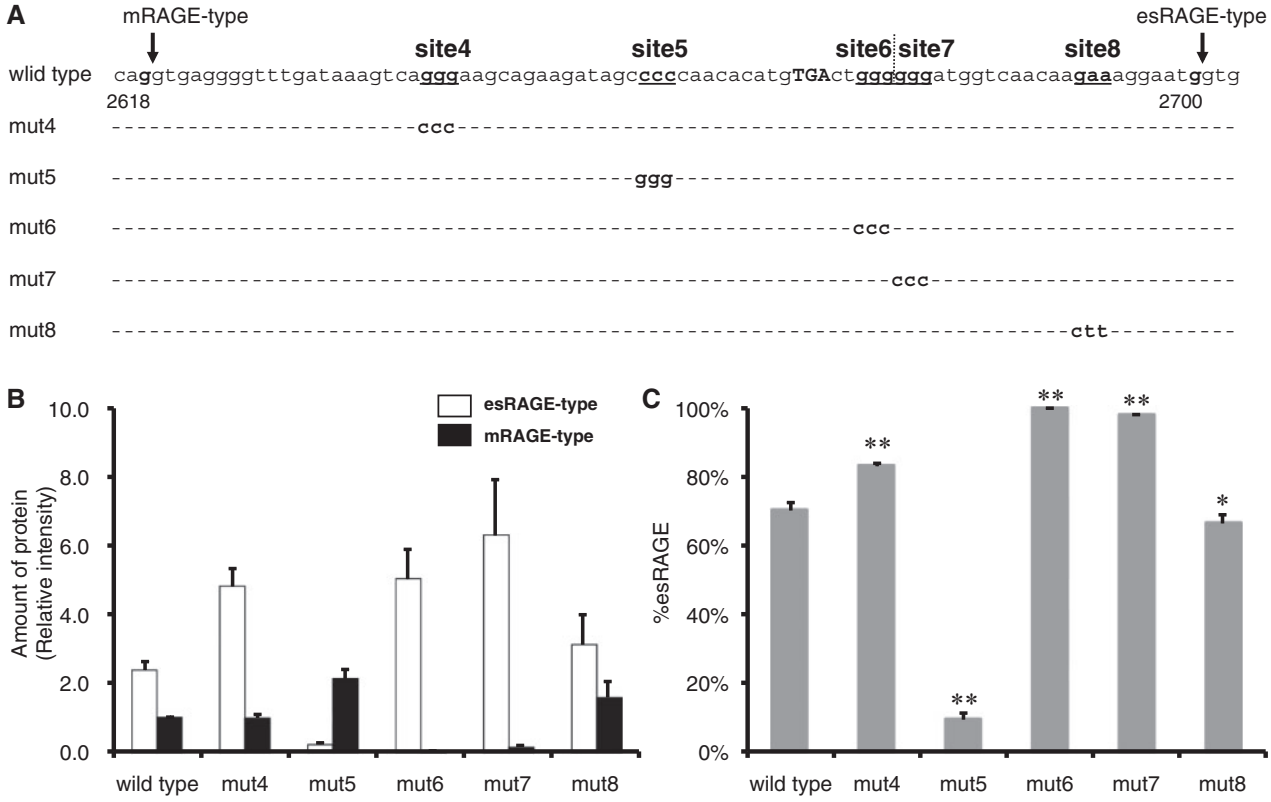

Fig. 3 Effects of mutagenesis in exon 9B on the alternative splicing in HEK293T. (A) Wild-type nucleotide sequence of exon 9B and the 5 mutations introduced into the minigene. Arrows indicate the 5′ splice sites of mRAGE- and esRAGE-type splicing. The last nucleotides of exon 9 and exon 9B are numbered (the nucleotide numbers are based on the genomic sequence starting from the first ATG of exon 1). Capitals 'TGA' indicate in-frame stop codon. In the wild-type sequence, nucleotides targeted for the substitutions are underlined. Dotted line between site 6 and site 7 indicates the boundary of the two target sites. (B) Quantification of esRAGE-type (open bar) and mRAGE-type (closed bar) protein products by western blotting using anti-GFP antibody. All data were normalized by the intensity of GAPDH used as an internal control. Bars indicate mean ± SD ($n=6$). (C) %esRAGE (percentage of esRAGE-type product in sum of esRAGE-type and mRAGE-type products) was calculated from (B). Bars indicate mean ±SD (**$P<0.01$; *$P<0.05$ versus wild-type).

Furthermore, we analysed the relative quantity of mRNA corresponding to mRAGE- and esRAGE-type by multiplex qRT-PCR using TaqMan probes (Fig. 4C and D). The %esRAGE of wild-type minigene-derived products was 11.8%, indicating that the mRAGE 5′ splice site is preferentially utilized. This was consistent with the results of qRT-PCR analysis of endogenous RAGE transcripts, in which the %esRAGE was 2.8% (Supplementary Fig. S2). The direction of the effect of each mutation on %esRAGE at the mRNA level was identical to that at the protein level. The three mutations mut4, mut6 and mut7, in which G-triplets were replaced by C-triplets, showed significant increases in %esRAGE (37.8% for mut4, 99.6% for mut6 and 80.8% for mut7) compared with the wild-type. Mutation mut5, in which a C-triplet was replaced by a G-triplet, showed a drastic decrease in %esRAGE to 0.1%. No significant effect of mut8 on the alternative splicing was observed.

It should be noted that the esRAGE/mRAGE ratios observed at the mRNA level were generally lower than those observed at the protein level in all minigene experiments. This could be at least partly ascribed to the rapid removal of mRAGE protein from the cell surface due to shedding by proteases (*21–23*).

hnRNP H Specifically Binds the G-Stretches in Exon 9B

Sites 6 and 7 comprise a 6-nucleotide G-stretch, and similar G-rich sequences have been identified as the signature of binding sites for hnRNP H family proteins (*24–26*). To assess the ability of hnRNP H to bind to this sequence, we examined complex formation of fluorescent dye-labelled RNA probes and hnRNP H in a nuclear extract of HEK293T cells by RIP followed by REMSA (Table II and Fig. 5). To minimize artifactual results caused by non-specific cross-reaction of the antibody, different anti-hnRNP H antibodies were used for the immunoprecipitation and for the western blotting.

Complex formation of hnRNP H and the RNA probe encompassing sites 6 and 7 was observed, and the binding disappeared following replacement of GGG by CCC at sites 6 and 7 (Fig. 5, sites 6–7). These results demonstrated that hnRNP H binds the wild-type sequence of sites 6–7, and that the G-stretch that resides therein is essential for the interaction. The importance of the G-stretch in exon 9B for the interaction with hnRNP H was further supported by the results with RNA probes encompassing site 5; the wild-type sequence did not bind hnRNP H, and replacement of CCC by GGG caused the binding of the RNA and hnRNP H (Fig. 5, site 5). Therefore,

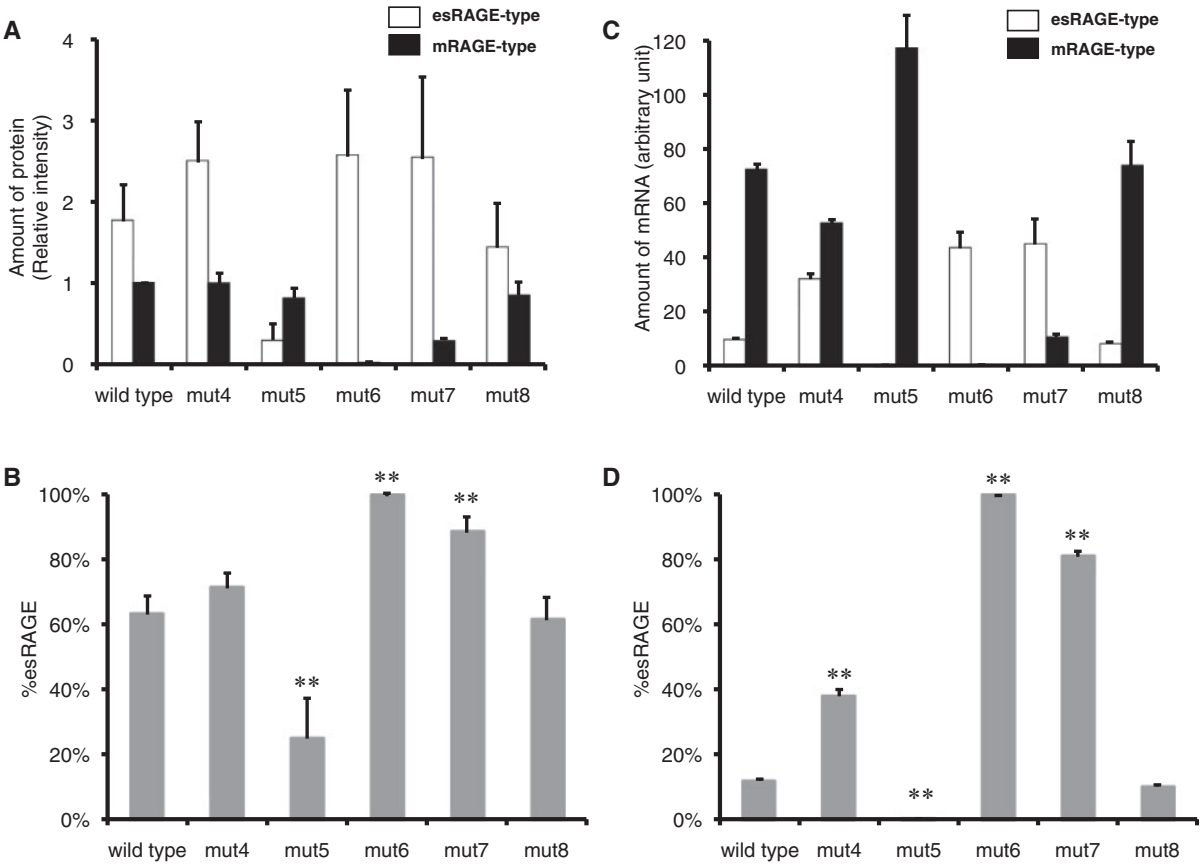

Fig. 4 Effects of mutagenesis in exon 9B on alternative splicing in HMVEC. (A) Quantification of esRAGE-type (open bar) and mRAGE-type (closed bar) protein products by western blotting using anti-GFP antibody. All data were normalized by the intensity of GAPDH used as an internal control. Bars indicate mean ± SD ($n=6$). (B) Values of %esRAGE at the protein level were calculated from (A). Bars indicate mean ± SD (**$P<0.01$ versus wild-type). (C) qRT-PCR quantification of esRAGE-type (open bar) and mRAGE-type (closed bar) RNA products. All data were normalized using GAPDH mRNA levels. Bars indicate mean ± SD ($n=3$). (D) Values for %esRAGE at the mRNA level were calculated from (C). Bars indicate mean ± SD (**$P<0.01$ versus wild-type).

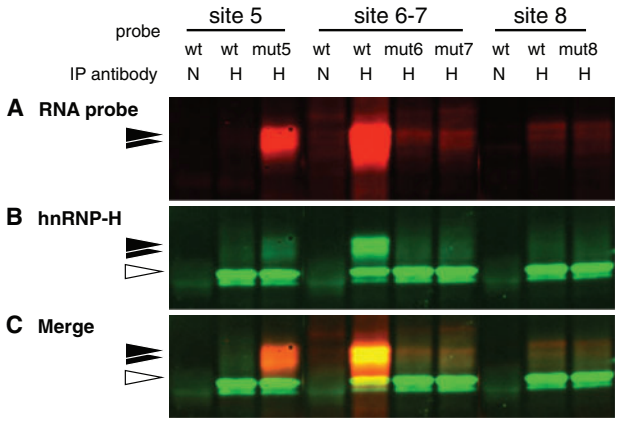

Fig. 5 hnRNP H binding to RNA sequences in exon 9B in a G-stretch-dependent manner. HEK293T cell nuclear extracts were subjected to RIP followed by REMSA with fluorescent dye-labelled RNA oligonucleotide probes (nucleotide sequences of probes are indicated in Table II). UV-crosslinked RNA–protein complexes were transferred to PVDF membrane and detected by anti-hnRNP H antibody using an Odyssey system. (A) Fluorescence of the RNA probes is shown in red. (B) The hnRNP H-immunoreactive bands are shown in green. (C) In overlay images of (A) and (B), the complex of the RNA probe and hnRNP H appeared as retarded yellow bands, and unbound hnRNP H appeared as fast migrating green bands. Closed arrowheads indicate RNA–protein complexes, and open arrowheads indicate unbound hnRNP H. *wt*, probe with wild-type sequence; *mut*, probe with mutations; *N*, IP with normal rabbit IgG; *H*, IP with anti-hnRNP H antibody.

these results indicated that hnRNP H binds to the RNA probe in a sequence-dependent manner, and that, in particular, the G-stretch is important for hnRNP H binding. The site 8 probe, either wild-type sequence or mutated sequence, barely bound with hnRNP H, probably due to the absence of the G-stretch (Fig. 5, site 8).

DISCUSSION

In this study, we identified G-rich *cis*-elements in exon 9B that are essential for the 5′ splice site selection in intron 9 of the RAGE pre-mRNA and demonstrated the involvement of hnRNP H as a regulatory protein that interacts with these *cis*-elements.

We introduced a series of 3-nucleotide substitutions to sites 4–8 in exon 9B of a RAGE minigene construct (Fig. 3A). The effects of each mutation on RAGE alternative splicing were similar between HEK293T cells (Fig. 3B and C) and HMVEC (Fig. 4). The mutations of the G-stretch at sites 6–7 nearly abrogated the production of mRAGE. Mutation of the G-triplet at site 4 also significantly decreased the mRAGE-type product but the effect was less than those for sites 6–7. Notably, the introduction of an additional G-triplet in place of a C-triplet at site 5 caused

preferential utilization of the mRAGE 5′ splice site. The number of G-triplets in exon 9B appeared to correlate with the extent of utilization of the mRAGE 5′ splice site. The results were similar to the case of artificially duplicated 5′ splice sites of the human α-globin gene intron 2, in which G-triplets flanked by the two alternative 5′ splice sites activate the upstream site and the number of the G-triplets correlated with the extent of the activation (*27*).

The sequences of the G-rich *cis*-elements identified in the present study, sites 4 and 6–7 matched the consensus motif of the binding site of hnRNP H family proteins, DGGGD (where D is U, G or A) (*24*). The hnRNP H family is composed of hnRNPs H1, H2, F, 2H9 and GRSF-1, which are highly homologous, ubiquitously expressed proteins that have RNA recognition motifs. They have been implicated in RNA processing such as splicing, polyadenylation, capping and transport of RNA (*24*). hnRNP H has also been reported to be involved in the regulation of 5′ splice site selection in Bcl-xS/Bcl-xL (*2*) and DM20/PLP (*28*, *29*). In both cases, the G-rich *cis*-elements were identified within the region between the two alternative 5′ splice sites, as in the case of G-rich *cis*-elements in RAGE exon 9B. The results of mutant minigene experiments in this study are in accord with the reports that the disruption of G-rich *cis*-elements abolished the binding of hnRNP H and led to preferential utilization of the downstream 5′ splice site in Bcl-xS/Bcl-xL (*2*) and in DM20/PLP transcripts (*29*).

To examine whether the G-rich *cis*-elements in exon 9B bind to hnRNP H, we carried out RIP followed by REMSA. The results of the binding assay clearly showed that the RNA probe encompassing the G-stretch at site 6–7 bound to hnRNP H. Continuity of the G-stretch may be important in this particular region because mutations at sites 6 (mut6) and 7 (mut7) resulted in drastic decreases in hnRNP H binding even though 3 out of the 6 guanine nucleotides in the stretch were still preserved in both mutated sequences (Fig. 5, sites 6–7). On the other hand, the introduction of a G-triplet in the place of a C-triplet at site 5 (mut5) conferred affinity for hnRNP H (Fig. 5, site 5). Although the mutated sequence at site 5, CGG GC does not match the best motifs for binding, an intermediate affinity by hnRNP H has been described (*24*).

Because the G-rich *cis*-elements in exon 9B were essential both for preferential utilization of the mRAGE 5′ splice site and for the binding to hnRNP H, we hypothesized that the *cis*-elements regulate 5′ splice site selection via interaction with hnRNP H, either by promoting utilization of the mRAGE 5′ splice site or inhibiting use of the esRAGE 5′ splice site.

The skipping of exon 10 in esRAGE-type splicing may be ascribed to the limitation of intron length in higher eukaryotes. Roughly 45 nucleotides must separate the 5′ splice site and branch point (*30–34*), and the minimum distance between the branch point and 3′ splice site appears to be ~18 nucleotides (*30*, *35*), respectively. Therefore introns shorter than 70 nucleotides are extremely rare in mammals and cannot be spliced out efficiently (*36*). When the esRAGE 5′ splice site in intron 9 is selected, the distance between this site and the 3′ splice site that borders exon 10 is 46 nucleotides, which is considerably shorter than the lower limit of the intron length. Therefore, the use of the downstream, esRAGE 5′ splice site of intron 9 and the inclusion of exon 10 would be mutually exclusive. This notion may be supported by the report by Hudson *et al.* (*37*), which analysed human RAGE splice variants. Among the 20 splice variants analysed, all variants that used the downstream esRAGE 5′ splice site in intron 9 skipped exon 10; in contrast, all variants that used the upstream mRAGE 5′ splice site in intron 9 included exon 10. Thus, the available evidence indicates that the selection of either one of the two alternative 5′ splice sites in intron 9 is the most likely the key event of RAGE alternative splicing, which couples with inclusion or exclusion of exon 10.

The regulation of RAGE alternative splicing is also important from the clinical viewpoint, because it has been suggested that RAGE signalling is involved in a wide range of pathologies and disorders, such as diabetes (*12*, *13*), Alzheimer's disease (*8*) and cancer (*11*), and because the balance of expressions of the two RAGE products generated by alternative splicing, cytotoxic mRAGE and cytoprotective esRAGE, is considered to be associated with susceptibility/resistance to these RAGE-related disorders. A few drugs have been reported to affect serum levels of esRAGE. Angiotensin converting enzyme-1 inhibitors (ACEI) purportedly increase esRAGE mRNA expression and decrease mRAGE mRNA expression in cultured bovine aortic endothelial cells and in the renal cortex of diabetic mice (*38*). An increase in esRAGE has been observed in ACEI-treated (*38*) and thiazolidinedione-treated diabetic patients (*39*). Elucidation of the regulatory mechanism of RAGE alternative splicing may pave the way for the development of drugs that can induce esRAGE but suppress mRAGE and could be promising candidates of preventive or curative medicines for RAGE-related disorders.

SUPPLEMENTARY DATA

Supplementary Data are available at JB Online.

Acknowledgements

The authors thank Dr Masatoshi Hagiwara at Tokyo Medical and Dental University Medical Research Institute and School of Biomedical Science for critical review of the manuscript; Mr Shin-ichi Matsudaira, Ms Reiko Kitamura and Ms Yuko Niimura for assistance; Mr Satoru Yoshida at Stratagene Products Division, Agilent Technologies Japan Ltd, for technical support in qRT-PCR, and Dr David Klein for reading the manuscript.

Funding

Grants-in-aid from the Japan Society for the Promotion of Sciences (nos.18590260, 19390085, 20590290, and 21590304); Project Research from the High-Technology Center of Kanazawa Medical University (to H.Y., H2009-10).

Conflict of interest

None declared.

References

1. Johnson, J.M., Castle, J., Garrett-Engele, P., Kan, Z., Loerch, P.M., Armour, C.D., Santos, R., Schadt, E. E., Stoughton, R., and Shoemaker, D.D. (2003) Genome-wide survey of human alternative pre-mRNA splicing with exon junction microarrays. *Science* **302**, 2141–2144
2. Garneau, D., Revil, T., Fisette, J.F., and Chabot, B. (2005) Heterogeneous nuclear ribonucleoprotein F/H proteins modulate the alternative splicing of the apoptotic mediator Bcl-x. *J. Biol. Chem.* **280**, 22641–22650
3. Yonekura, H., Yamamoto, Y., Sakurai, S., Petrova, R.G., Abedin, M.J., Li, H., Yasui, K., Takeuchi, M., Makita, Z., Takasawa, S., Okamoto, H., Watanabe, T., and Yamamoto, H. (2003) Novel splice variants of the receptor for advanced glycation end-products expressed in human vascular endothelial cells and pericytes, and their putative roles in diabetes-induced vascular injury. *Biochem. J.* **370**, 1097–1109
4. Harashima, A., Yamamoto, Y., Cheng, C., Tsuneyama, K., Myint, K.M., Takeuchi, A., Yoshimura, K., Li, H., Watanabe, T., Takasawa, S., Okamoto, H., Yonekura, H., and Yamamoto, H. (2006) Identification of mouse orthologue of endogenous secretory receptor for advanced glycation end-products: structure, function and expression. *Biochem. J.* **396**, 109–115
5. Neeper, M., Schmidt, A.M., Brett, J., Yan, S.D., Wang, F., Pan, Y.C., Elliston, K., Stern, D., and Shaw, A. (1992) Cloning and expression of a cell surface receptor for advanced glycosylation end products of proteins. *J. Biol. Chem.* **267**, 14998–15004
6. Schmidt, A.M., Yan, S.D., Yan, S.F., and Stern, D.M. (2001) The multiligand receptor RAGE as a progression factor amplifying immune and inflammatory responses. *J. Clin. Invest.* **108**, 949–955
7. Hofmann, M.A., Drury, S., Fu, C., Qu, W., Taguchi, A., Lu, Y., Avila, C., Kambham, N., Bierhaus, A., Nawroth, P., Neurath, M.F., Slattery, T., Beach, D., McClary, J., Nagashima, M., Morser, J., Stern, D., and Schmidt, A.M. (1999) RAGE mediates a novel proinflammatory axis: a central cell surface receptor for S100/calgranulin polypeptides. *Cell* **97**, 889–901
8. Yan, S.D., Chen, X., Fu, J., Chen, M., Zhu, H., Roher, A., Slattery, T., Zhao, L., Nagashima, M., Morser, J., Migheli, A., Nawroth, P., Stern, D., and Schmidt, A.M. (1996) RAGE and amyloid-β peptide neurotoxicity in Alzheimer's disease. *Nature* **382**, 685–691
9. Chavakis, T., Bierhaus, A., Al-Fakhri, N., Schneider, D., Witte, S., Linn, T., Nagashima, M., Morser, J., Arnold, B., Preissner, K.T., and Nawroth, P.P. (2003) The pattern recognition receptor (RAGE) is a counterreceptor for leukocyte integrins: a novel pathway for inflammatory cell recruitment. *J. Exp. Med.* **198**, 1507–1515
10. Hori, O., Brett, J., Slattery, T., Cao, R., Zhang, J., Chen, J.X., Nagashima, M., Lundh, E.R., Vijay, S., Nitecki, D., Moser, J., Stern, D., and Schmidt, A.M. (1995) The receptor for advanced glycation end products (RAGE) is a cellular binding site for amphoterin. Mediation of neurite outgrowth and co-expression of rage and amphoterin in the developing nervous system. *J. Biol. Chem.* **270**, 25752–25761
11. Taguchi, A., Blood, D.C., del Toro, G., Canet, A., Lee, D.C., Qu, W., Tanji, N., Lu, Y., Lalla, E., Fu, C., Hofmann, M.A., Kislinger, T., Ingram, M., Lu, A., Tanaka, H., Hori, O., Ogawa, S., Stern, D.M., and Schmidt, A.M. (2000) Blockade of RAGE-amphoterin signalling suppresses tumour growth and metastases. *Nature* **405**, 354–360
12. Myint, K.M., Yamamoto, Y., Doi, T., Kato, I., Harashima, A., Yonekura, H., Watanabe, T., Shinohara, H., Takeuchi, M., Tsuneyama, K., Hashimoto, N., Asano, M., Takasawa, S., Okamoto, H., and Yamamoto, H. (2006) RAGE control of diabetic nephropathy in a mouse model: effects of RAGE gene disruption and administration of low-molecular weight heparin. *Diabetes* **55**, 2510–2522
13. Yamamoto, Y., Kato, I., Doi, T., Yonekura, H., Ohashi, S., Takeuchi, M., Watanabe, T., Yamagishi, S., Sakurai, S., Takasawa, S., Okamoto, H., and Yamamoto, H. (2001) Development and prevention of advanced diabetic nephropathy in RAGE-overexpressing mice. *J. Clin. Invest.* **108**, 261–268
14. Koyama, H., Shoji, T., Yokoyama, H., Motoyama, K., Mori, K., Fukumoto, S., Emoto, M., Tamei, H., Matsuki, H., Sakurai, S., Yamamoto, Y., Yonekura, H., Watanabe, T., Yamamoto, H., and Nishizawa, Y. (2005) Plasma level of endogenous secretory RAGE is associated with components of the metabolic syndrome and atherosclerosis. *Arterioscler. Thromb. Vasc. Biol.* **25**, 2587–2593
15. Sakurai, S., Yamamoto, Y., Tamei, H., Matsuki, H., Obata, K., Hui, L., Miura, J., Osawa, M., Uchigata, Y., Iwamoto, Y., Watanabe, T., Yonekura, H., and Yamamoto, H. (2006) Development of an ELISA for esRAGE and its application to type 1 diabetic patients. *Diabetes. Res. Clin. Pract.* **73**, 158–165
16. Sugaya, K., Fukagawa, T., Matsumoto, K., Mita, K., Takahashi, E., Ando, A., Inoko, H., and Ikemura, T. (1994) Three genes in the human MHC class III region near the junction with the class II: gene for receptor of advanced glycosylation end products, PBX2 homeobox gene and a notch homolog, human counterpart of mouse mammary tumor gene int-3. *Genomics* **23**, 408–419
17. Ito, W., Ishiguro, H., and Kurosawa, Y. (1991) A general method for introducing a series of mutations into cloned DNA using the polymerase chain reaction. *Gene* **102**, 67–70
18. Dignam, J.D. (1990) Preparation of extracts from higher eukaryotes. *Methods. Enzymol.* **182**, 194–203
19. Mount, S.M., Pettersson, I., Hinterberger, M., Karmas, A., and Steitz, J.A. (1983) The U1 small nuclear RNA-protein complex selectively binds a 5′ splice site *in vitro*. *Cell* **33**, 509–518
20. Yu, Y., Maroney, P.A., Denker, J.A., Zhang, X.H., Dybkov, O., Luhrmann, R., Jankowsky, E., Chasin, L.A., and Nilsen, T.W. (2008) Dynamic regulation of alternative splicing by silencers that modulate 5′ splice site competition. *Cell* **135**, 1224–1236
21. Galichet, A., Weibel, M., and Heizmann, C.W. (2008) Calcium-regulated intramembrane proteolysis of the RAGE receptor. *Biochem. Biophys. Res. Commun.* **370**, 1–5
22. Raucci, A., Cugusi, S., Antonelli, A., Barabino, S.M., Monti, L., Bierhaus, A., Reiss, K., Saftig, P., and Bianchi, M.E. (2008) A soluble form of the receptor for advanced glycation endproducts (RAGE) is produced by proteolytic cleavage of the membrane-bound form by the sheddase a disintegrin and metalloprotease 10 (ADAM10). *FASEB J.* **22**, 3716–3727
23. Zhang, L., Bukulin, M., Kojro, E., Roth, A., Metz, V.V., Fahrenholz, F., Nawroth, P.P., Bierhaus, A., and Postina, R. (2008) Receptor for advanced glycation end products is subjected to protein ectodomain shedding by metalloproteinases. *J. Biol. Chem.* **283**, 35507–35516
24. Schaub, M.C., Lopez, S.R., and Caputi, M. (2007) Members of the heterogeneous nuclear ribonucleoprotein H family activate splicing of an HIV-1 splicing

substrate by promoting formation of ATP-dependent spliceosomal complexes. *J. Biol. Chem.* **282**, 13617–13626
25. Caputi, M. and Zahler, A.M. (2001) Determination of the RNA binding specificity of the heterogeneous nuclear ribonucleoprotein (hnRNP) H/H'/F/2H9 family. *J. Biol. Chem.* **276**, 43850–43859
26. Honoré, B., Rasmussen, H.H., Vorum, H., Dejgaard, K., Liu, X., Gromov, P., Madsen, P., Gesser, B., Tommerup, N., and Celis, J.E. (1995) Heterogeneous nuclear ribonucleoproteins H, H', and F are members of a ubiquitously expressed subfamily of related but distinct proteins encoded by genes mapping to different chromosomes. *J. Biol. Chem.* **270**, 28780–28789
27. McCullough, A.J. and Berget, S.M. (1997) G triplets located throughout a class of small vertebrate introns enforce intron borders and regulate splice site selection. *Mol. Cell. Biol.* **17**, 4562–4571
28. Wang, E. and Cambi, F. (2009) Heterogeneous nuclear ribonucleoproteins H and F regulate the proteolipid protein/DM20 ratio by recruiting U1 small nuclear ribonucleoprotein through a complex array of G runs. *J. Biol. Chem.* **284**, 11194–11204
29. Wang, E., Dimova, N., and Cambi, F. (2007) PLP/DM20 ratio is regulated by hnRNPH and F and a novel G-rich enhancer in oligodendrocytes. *Nucleic. Acids. Res.* **35**, 4164–4178
30. Fu, X.Y., Colgan, J.D., and Manley, J.L. (1988) Multiple cis-acting sequence elements are required for efficient splicing of simian virus 40 small-t antigen pre-mRNA. *Mol. Cell. Biol.* **8**, 3582–3590
31. Ruskin, B., Greene, J.M., and Green, M.R. (1985) Cryptic branch point activation allows accurate *in vitro* splicing of human β-globin intron mutants. *Cell* **41**, 833–844
32. Smith, C.W. and Nadal-Ginard, B. (1989) Mutually exclusive splicing of α-tropomyosin exons enforced by an unusual lariat branch point location: implications for constitutive splicing. *Cell* **56**, 749–758
33. Ulfendahl, P.J., Pettersson, U., and Akusjarvi, G. (1985) Splicing of the adenovirus-2 E1A 13S mRNA requires a minimal intron length and specific intron signals. *Nucleic. Acids. Res.* **13**, 6299–6315
34. Wieringa, B., Hofer, E., and Weissmann, C. (1984) A minimal intron length but no specific internal sequence is required for splicing the large rabbit β-globin intron. *Cell* **37**, 915–925
35. Reed, R. and Maniatis, T. (1985) Intron sequences involved in lariat formation during pre-mRNA splicing. *Cell* **41**, 95–105
36. Mount, S.M., Burks, C., Hertz, G., Stormo, G.D., White, O., and Fields, C. (1992) Splicing signals in Drosophila: intron size, information content, and consensus sequences. *Nucleic. Acids. Res.* **20**, 4255–4262
37. Hudson, B.I., Carter, A.M., Harja, E., Kalea, A.Z., Arriero, M., Yang, H., Grant, P.J., and Schmidt, A.M. (2008) Identification, classification, and expression of RAGE gene splice variants. *FASEB J.* **22**, 1572–1580
38. Forbes, J.M., Thorpe, S.R., Thallas-Bonke, V., Pete, J., Thomas, M.C., Deemer, E.R., Bassal, S., El-Osta, A., Long, D.M., Panagiotopoulos, S., Jerums, G., Osicka, T.M., and Cooper, M.E. (2005) Modulation of soluble receptor for advanced glycation end products by angiotensin-converting enzyme-1 inhibition in diabetic nephropathy. *J. Am. Soc. Nephrol.* **16**, 2363–2372
39. Tan, K.C., Chow, W.S., Tso, A.W., Xu, A., Tse, H.F., Hoo, R.L., Betteridge, D.J., and Lam, K.S. (2007) Thiazolidinedione increases serum soluble receptor for advanced glycation end-products in type 2 diabetes. *Diabetologia* **50**, 1819–1825